Life Science Informatics Publications

Research Journal of Life Sciences, Bioinformatics, Pharmaceutical and Chemical Sciences

Journal Home page http://www.rjlbpcs.com/

RJLBPCS

ISSN 2454-6348

Original Research Article **DOI - 10.26479/2016.0201.02**

NOVEL INSIGHTS INTO THE STRUCTURAL MECHANISMS OF FEXB PROTEIN RESISTANCE TOWARDS CHLORAMPHENICOL: A BIOINFORMATICS APPROACH

Hemalatha Golaconda Ramulu*

School of Chemistry, University of Hyderabad, Telangana, Hyderabad 500046, India

ABSTRACT: Chloramphenicol (Clm) is one of the most widely used broad spectrum antibiotic in veterinary medicine. Recent studies have shown that there is a development of an acquired resistance against Clm by FexB protein which is encoded by its *fexB* phenicol resistant gene. However, the structural mechanism of its antibiotic resistance towards Clm is unknown due to lack of structural data on FexB protein. Therefore, we have build a 3D structural model of FexB protein using MdfA as template structure by homology modeling and validated it by structure-verification programs. This was followed by binding pocket analysis, molecular docking and molecular dynamic (MD) simulations. Docking results showed the presence of intermolecular hydrogen bonding of Clm with THR151 amino acid residue and changes in the binding orientation of Clm. Analysis from MD simulations revealed significant differences in conformational dynamics of Clm binding in FexB model when compared to MdfA. Our analysis showed that despite of FexB structural similarity with MdfA, it also revealed some distinct features such as mutation of ALA30 and SER93 amino acid residues and large substrate binding pocket that may play important role in contributing its resistance towards Clm. Our detailed data analysis on the FexB protein model and its interactions with Clm on a structural basis is novel and has not been reported earlier. We believe that our work will provide a significant insight in designing more potent inhibitors against antibiotic-resistant FexB protein.

KEYWORDS: Phenicol resistant gene, FexB protein, Chloramphenicol, antibiotic resistance, Homology modeling, Molecular Docking, Molecular dynamics.

***Corresponding Author: Dr. Hemalatha Golaconda Ramulu** Ph. D.

School of Chemistry, University of Hyderabad, Telangana, Hyderabad 500046, India,

*Email Address: hema1752002@gmail.com

1. INTRODUCTION

Resistance to antibiotics has emerged as a global health problem. The contributing factors for antibiotic resistance in micro-organisms are as follows: Drug alteration/inactivation, target modification thereby reducing the drug accumulation and portability by increasing the resistance mechanism [1-3]. Other factors like mutations, transfer of resistance genes by mobile genetic elements from one organism to another by horizontal gene transfer [4-5] will also play a significant role towards antibiotic resistance. Antibiotics have been used extensively among cattle, poultry, in aquaculture for different purposes such as growth promoters, for treatment of infections. This has lead to an increase in the selective pressure on both commensal and pathogenic micro-organisms and eventually antibiotics use has disseminated in the food chain and environment from the industrial pollution emissions, thus affecting humans and other micro-organisms [6]. Among them, Clm and Florfenicol(Ff) are widely used as broad spectrum antibiotics in veterinary medicine. Clm, originally known as chloromycetin, was isolated from *Streptomyces venezuelae* in 1947 [7] and was used in cadaver of food animals. Due to number of adverse effects with its use such as dose-unrelated irreversible aplastic anemia [8] and Gray syndrome (dose-related reversible bone-marrow suppression) in newborns and infants [9-10], it is prohibited in food producing animals and human medicine. It has been reported that Ff which was derived from fluorinated chloramphenicol and does not cause any toxic effects, therefore it is used as a therapy for bacterial respiratory infections in food producing animals [11]. Both Clm and Ff inhibit protein translation in bacteria by acting at the centres of 50S ribosomes of peptidyl transferase [12]. With the exclusive use of antibiotics, we have witnessed a drastic increase in several bacterial pathogens that have been resistant towards them. Recently, two new species, i.e., *Enterococcus faecium* EFM-1 and *Enterococcus hirae* EH-1 were identified that have conferred resistance to Clm and Ff. The two resistant species were isolated from nasal swabs of porcine origin and carried a novel phenicol resistance gene, called as *fexB.* The *fexB* gene was located on the plasmids in both *Enterococcus* species and codes for FexB protein that consists of 469 amino acids with 14 transmembrane domains. FexB protein confers resistance to Clm and Ff and shares amino acid similarity of 56.1% with FexA and 15.6% with PexA protein sequences [13]. The structural data on FexB protein has not been reported till date. Therefore, in the current study we aim to build the three dimensional (3D) structure of FexB protein using homology modeling and dock the Clm into the binding pocket by molecular docking to analyze its interactions in FexB

model. Further, we have carried out Molecular dynamic (MD) simulations of the protein–ligand complex to decipher the structural basis of FexB protein resistance towards Clm. To our knowledge, this is the first elucidated structure of FexB protein, based on which more potent drugs may be designed that can be effective against Clm antibiotic resistant micro-organisms.

2. MATERIALS AND METHODS

2.1 Sequence Analysis

The amino acid sequence of FexB protein encoded by novel phenicol *fexB* gene was retrieved from the NCBI database (Accession ID: AEV23046.1) and submitted for the prediction of transmembrane domains using Tmpred program (http://www.ch.embnet.org/software/TMPREDform.html) [14]. As the information on FexB protein is unavailable, we have calculated its physicochemical properties by *in silico* method using the ProtParam tool of the ExPASy server [15]. The arrangement of secondary structural elements of FexB protein sequence was predicted using PDBsum server [16]. Additionally, we have also analyzed other characteristics such as stability and charge of folding and unfolding state including pH of FexB and MdfA proteins using PROPKA 3.0 software [17]. The electrostatic potentials of both protein surfaces were calculated from the Poisson–Boltzmann electrostatics calculations of PDB2PQR server [18] via Adaptive Poisson-Boltzmann solver (APBS) [19] (http://nbcr-22.ucsd.edu/pdb2pqr2 .0.0/) by default parameters.

2.2 Homology Modeling

Homology modeling, also known as comparative modeling, is a method that is employed for building the protein model from its amino acid sequence based on the homology of experimentally determined structure. We have retrieved the FexB protein sequence (Accession ID: AEV23046.1) from the NCBI database (http://www.ncbi.nlm.nih.gov/) and submitted to BLAST algorithm [20] against Protein Data Bank (PDB) [21] to carry out the sequence homology search. The BLAST homology search identified MdfA (PDB ID: 4ZOW) as template structure, which is a multidrug resistant transporter protein from *Escherichia coli* (*E.coli)* with Clm complex [22] and it was used as template for homology modeling. The sequences of template and target protein were aligned using Clustal Omega [23], with David Arthur's k-means ++ code [24] for fast clustering of sequence vectors. The protein 3D structure of FexB protein was modeled using I-TASSER at (http://zhang.bioinformatics.ku.edu/I-TASSER/) [25]. I-TASSER builds structural models using suitable PDB by iterative fragment assembly approaches followed by functional prediction with known proteins from the function

databases. From the generated models, the structure model that was build based on the template sequence of MdfA (PDB ID: 4ZOW) was selected as the FexB 3D model, as the main objective of this project was to infer structural insights of FexB protein resistance towards Clm. Moreover, MdfA is the only available crystal structure with Clm complex till date.

2.3 Structural validation of predicted FexB model

We have used various structure validation methods such as VADAR 1.5(Volume Area Dihedral Angle Reporter) [26], followed by PROCHECK [27] and Verify_3D [28] for validating the quality of constructed FexB 3D model. VADAR 1.5 program (http://vadar.wishartlab.com/) provides the qualitative information of the modeled protein, that include mean hydrogen bonding distance and hydrogen bond energies, steric quality, accessible surface area, excluded volume, backbone and side chain dihedral angles, secondary structure, local and overall fold quality including solvation free energy. The results thus obtained were used for analyzing the quality of the modeled protein structure. PROCHECK calculates backbone conformation of the protein model by analysing the torsion angles and position in the Ramachandran plot [29]. Verify_3D evaluates the compatibility of FexB 3D structure model with its amino acid sequence. We have accessed PROCHECK and Verify_3D software services through online SAVES server (http://nihserver.mbi.ucla.edu/ SAVES/).

2.4 Prediction of Binding pocket

In order to dock the ligand in the FexB 3D model, it is important to determine its binding pocket. Therefore, we have used CASTp program [30] (Computed Atlas of Surface Topography of Proteins) for prediction of binding pocket of FexB 3D model and its template structure MdfA, and compared the conserved active site residues between them. This was used as guide for docking Clm ligand.

2.5 Molecular Docking

Docking was carried out using AutoDock Vina version 1.1[31]. Autodock Vina is considered to be more efficient than Autodock 4. The PDBQT files of the protein and ligand were prepared using AutodockTools 1.5.4 and all polar hydrogens were added to the molecules. We have used Broyden-Fletcher-Goldfarb-Shanno method in AutoDock Vina for local optimization and carried out docking by keeping the protein structures in rigid state while allowing full flexibility for ligand to rotate freely around all active torsions during docking. The following parameters were used: XYZ grid dimensions for MdfA 65.50 x 60.64 x 70.68; FexB model 63.50 x 59.64 x 69.68; exhaustiveness of the global search=8; maximum energy difference between the best binding mode and the worst=4; Binding

modes=10. The best binding mode of ligand from each docking run was analyzed based on docking score followed by visual evaluation using Discovery Studio 3.5 visualizer to analyze the mode of protein-ligand binding.

2.6 MD simulations

We have used GROMACS 4.5.4 package [32-33] with Gromo43a1 force fields for MD simulations. The best orientation of the docked ligand with the protein complexes of FexB and crystal structure MdfA were analyzed for conformational changes. The ligand input files were prepared using Dundee PRODRG server and protein–ligand complex was solvated using TIP3P water model using 10-Å cubic water box. Subsequently, in order to diffuse the water molecules throughout the system, we applied 1000 ps position-restrained dynamics and performed energy minimization of the complexes for 5000 steps of steepest descent followed by 5000 steps of conjugate gradient. This was followed by equilibration of protein-ligand complex using both NVT [34] run followed by NPT [35] at 298 K at 1 atmosphere. Finally, after equilibration, we have subjected the whole system to MD simulations for 10 ns. We employed LINCS algorithm [36] to constrain hydrogen bonds and particle-mesh Ewald (PME) algorithm [37-38] for electrostatic calculations that included short and long-range interactions. The trajectories obtained from MD simulations were analyzed using GROMACS analysis tools and VMD 1.9.2 [39].

3. RESULTS AND DISCUSSION

3.1 Conservation and variation in the sequences

The FexB protein has 469 amino acid sequence length and consists of 14 trans membrane domains (Fig.S1) as per Tmpred prediction. The pair wise sequence alignment of FexB protein sequence with MdfA showed the presence of conserved active site residues, along with some insertions as shown in Fig.1. The active site residues that were involved in Clm binding in MdfA are TYR30, ASP34, GLU26, ASN33, MET58, ILE122, MET146, ALA150, ALA153, PRO154 and ILE239. Among them, ASP31, LEU62, ILE247 and LEU302 were conserved in FexB along with other conserved residues. The amino acid sequence of FexB was 22% identical to MdfA. The analysis also revealed some important aspects with respect to the Clm binding such as presence of ALA30 and SER93 residues in FexB that were at equivalent position to ASN33 and CYS96 in MdfA. The mutational studies on Clm binding has shown that ASN33 to ALA and CYS96 to SER lost most of the binding

ability towards Clm[13]. Therefore, it can be predicted that the mutation of ALA30 and SER93 residues in FexB protein may affect its binding towards Clm.

3.1.1 *Conserved motifs*

We identified the following three conserved motifs in FexB, i.e. Motif B, C and D that were present in MFS antiporters[40] including MdfA orthologs [13].

Motif-B: It is designated by "R^{112}xxQG" consensus sequence in MdfA orthologs and is present in the N-terminal domain. It is the only motif with membrane-embedded basic residue among MFS members which is also termed as 3D motif-B [13]. We observed that motif-B (R^{109}mf$Q^{112}G^{112}$) was also conserved in FexB protein (Fig.1) and is located on helix-5 (Fig. S2). Among the residues, ARG112 plays an important role in carrying point mutations at position 112 in MdfA and the residue at ARG109 that is conserved in FexB may also be involved in similar activity. Along with ARG109, other residues such as GLN112 and GLY113 were also conserved in FexB protein. Motif-B was found to be important in the transfer of motif-B antiporters along with addition of protonation status with substrate binding in MdfA[13] and we predict a similar function for motif-B in FexB protein.

***Motif-C*:** Motif-C is formed by "itALMANvaLiaP^{154}LlGP^{158}LvG" consensus sequence in MdfA orthologs[13].It is located in rocker helix of Transmembrane5(TM5) ("$GX_6GX_3GPX_2GPX_2$ G") and is also called as antiporter motif [41]. We identified the "I^{139}LGIIA^{144}GCIGVGTAGG$^{154}P^{155}$IFG^{158}" consensus sequence as motif-C in FexB that is present on helix-6 region (Fig. S2). The PRO158 of motif-C was conserved among MdfA orthologs [13] and we have seen that the equivalent Proline residue at 155 (PRO155) is also conserved in motif-C of FexB protein along with I139, ALA144, GLY154 and GLY158 (Fig.1). It has been observed that the major part of C-terminal of motif-C (AG$G^{154}P^{155}$IFG^{158}) in FexB is largely conserved when compared to N-terminal half, which is in accordance to the previously reported results on motif-C of MdfA[13]. Motif-C of MdfA was involved in stabilizing the hydrophobic inter-domain interaction of MFS antiporters[13] and a similar activity can be predicted for motif-C in FexB protein.

***Motif-D*:** Motif-D is observed to form "E^{26}fxxY^{30}ianD^{34}miqP^{38}g" pattern and is present in TM1 in MdfA. It has been observed that the two acidic residues, i.e. ASP34 is absolutely conserved in MdfA transporters and GLU26 is conserved in majority (app. 80%) of known sequences [42]. The motif-D in FexB is formed by "VLVGSVTA$D^{31}M^{32}$VN$P^{35}V^{36}$" sequence pattern (Fig.1) located on helix-1(Fig.S2). We have observed that the acidic residue ASP31 is also conserved in FexB as seen in

MdfA. Apart from ASP31, MET32, PRO35 and VAL36 were also conserved in FexB. Motif-D plays a vital role in MdfA functions [43-45].

From the above analysis, we conclude that in FexB protein, motif-B is totally conserved whereas motif-C and D are partially conserved.

Fig.1 Pairwise sequence alignment of full length FexB and MdfA proteins. Active site residues in MfdA are highlighted in red and green arrow in FexB. Mutated residues in FexB are shown in cyan. Every 10th residue is numbered as per MdfA sequence. The significant conserved motifs i.e.Motifs D, B and C are indicated in boxes

3.1.2 Secondary structure and Physicochemical Properties

The secondary structure prediction from PDBsum server [16] revealed that FexB protein sequence mainly consists of alpha-helices (Fig.S2) indicating that the protein belongs to class of Major Facilitator Superfamily (MFS) of proteins. From the prediction of *in silico* physicochemical analysis, we have observed that the predicted extinction coefficients (ε) of FexB protein was low (31,525 M^{-1} cm^{-1}) when compared to MdfA (70,150 M^{-1} cm^{-1}). The instability indices (II) of FexB and MdfA were below 40, showing their more stability in solution. The GRAVY scores of both the proteins were positive, which indicates they both are soluble and exist in hydrophobic environments. However, the score of FexB was more (1.06) when compared to MdfA (0.86), which shows its soluble nature in more hydrophobic conditions. The aliphatic index (AI) was high for FexB protein (143.33) (signifying that it has increased thermo stability) when compared to MdfA (131.53) (Table 1).

Table.1 Computation of the physicochemical parameters of MdfA and FexB model

	Number of residues	MW	ε	II	AI	GRAVY	Asp+Glu	Arg+Lys
MdfA	391	42363.8	70,150	34.72	131.53	0.89	18	24
FexB	469	49216.0	31,525	27.76	143.33	1.06	14	22

MW molecular weight(g/mol), *ε* extinction coefficient(M^{-1} cm^{-1}), *II* instability index, *AI* aliphatic index, *GRAVY* grand average hydropathy, *Asp+Glu* number of negatively charged residues, *Arg+Lys* number of positively charged residues. Further, we have also analyzed other properties like the stability (free energy of folding) vs pH of both proteins and observed that FexB protein had the ideal pH of 9.4 with free energy of 18.4 kcal/mol at 298 K (Fig. 2a) whereas for MdfA, ideal pH and free energy were found to be 4.2 and 14.4 kcal/mol at 298 K (Fig. 2b) respectively. From the above analysis it is evident that FexB protein is favourable to basic pH. We found minor difference between the pIs of the two proteins from the analysis of folded and unfolded states vs pH. For FexB, they were 9.68 (folded) and 9.64 (unfolded) (Fig. 2c), whereas for MdfA, they were 10.13 (folded) and 9.34 (unfolded) (Fig. 2d). The electrostatic surface potential of FexB model and MdfA (Fig. S3a) from PDB2PQR server [18] revealed some variation in FexB model particularly at the C-terminal part that was negatively charged. Besides this, two small negatively charged grooves were also identified in the middle region of FexB model (Fig. S3b).

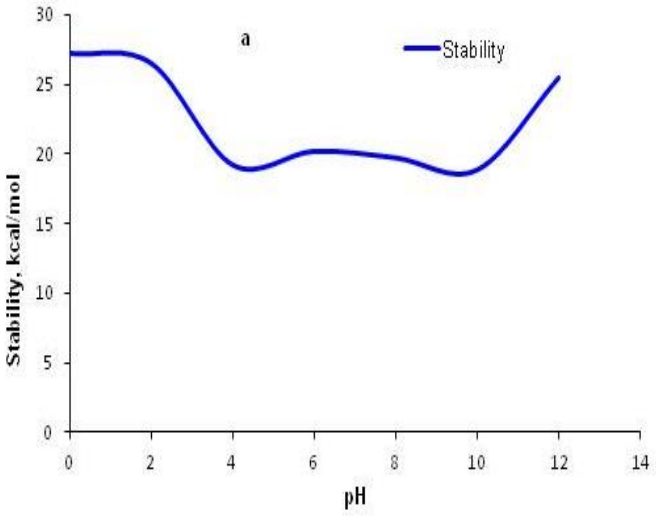

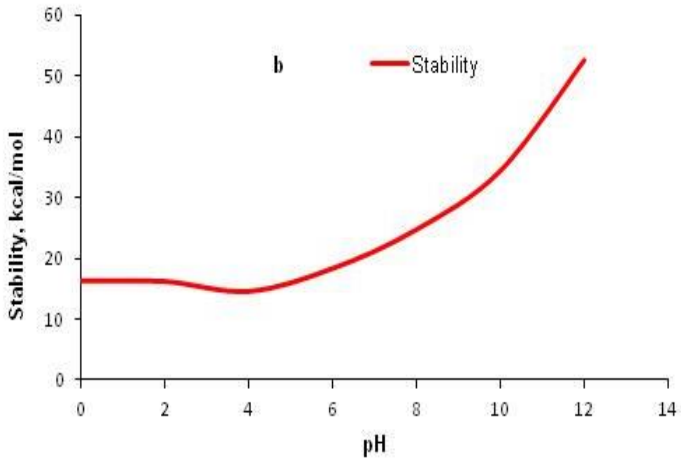

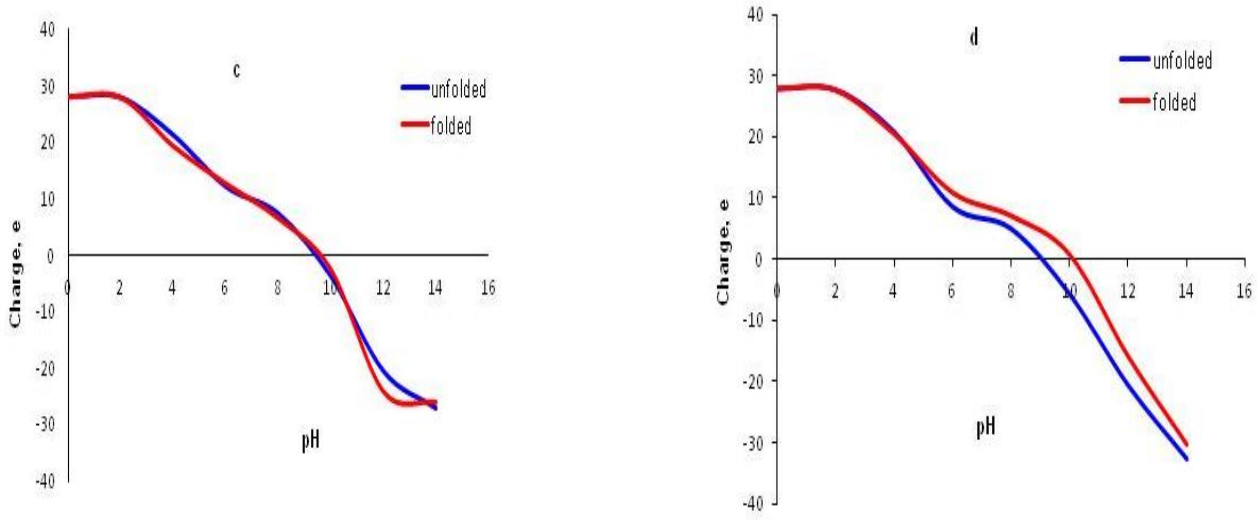

Fig.2 Effect of pH on the free energy of folding and charge of FexB protein and MdfA. The free energy of folding (stability) and the charge of the folding and unfolded states of FexB (**a** and **c**) and MdfA(**b** and **d**) were plotted as a function of pH. The plots were generated using PROPKA 3.0 [17]

3.2 Structural analysis of homology model

The homology model was generated using I-D TASSER using the crystal structure of MdfA, which is a substrate-bound multidrug resistant transporter protein from *E.coli* as the template. The preliminary FexB model thus obtained was further refined using energy minimization techniques. The refined and optimized model was validated by Ramachandran plot, PROCHECK, Verfiy3D, and ERRAT of SAVES server. From the Ramachandran plot, it has been observed that 81.1 % of the residues of FexB model were located in the allowed region with only 2.0 % in the disallowed region (Table 2, Fig. 3a); whereas the corresponding values for the MdfA were 97.3 % and 0.0 % respectively (Table 2, Fig. 3b). In addition, the overall quality factor of FexB model from ERRAT was found to be 86.768 and 61.62 % of residues had average 3D-1D score >0.2 from Verify3D (Table 2). The overall quality from G-factor quality was −0.57. From the above results, it is evident that FexB model was reliable and of good quality.

Fig.3 Ramachandran plot of the two proteins calculated using PROCHECK [23] (**a)** FexB model; (**b)** MdfA

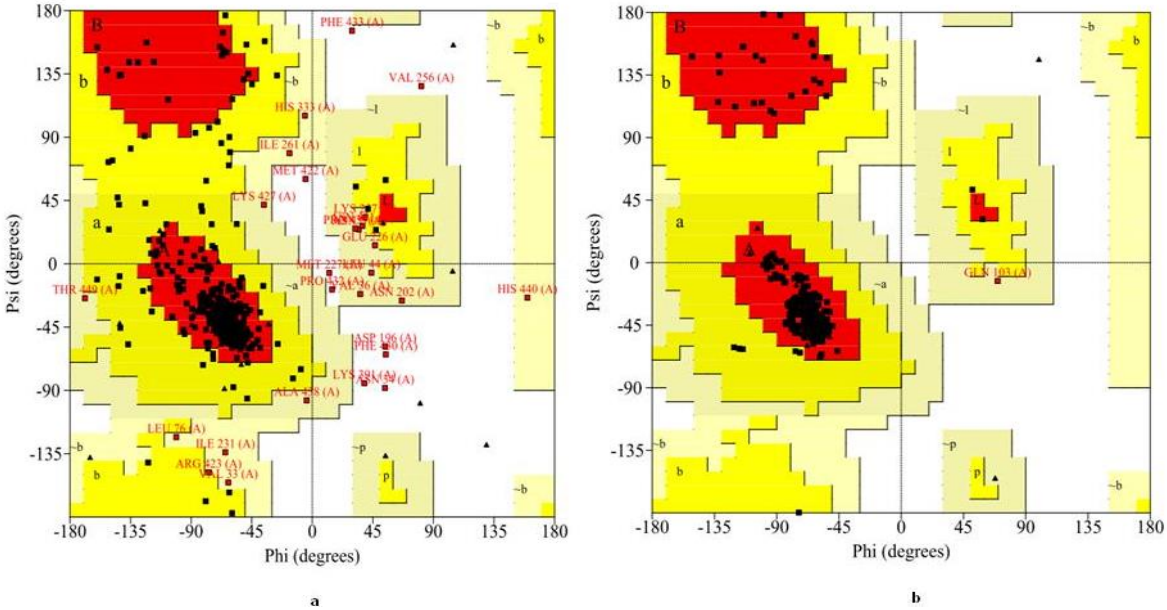

Table.2 Validation of the MdfA and FexB model by SAVES server

Protein	PROCHECK	Ramachandran plot				ERRAT	Verify3D
	G-factor	MFR	AAR	GAR	DAR		
MdfA	0.36	97.3 %	2.4%	0.3%	0.0%	97.911	87.98%
FexB	-0.57	81.1 %	12.5%	4.3%	2.0%	86.768	61.62%

MFR- Most favoured region; AAR- Additionally allowed region; GAR- Generously allowed region; DAR- Disallowed region

3.2.1 Model packing architecture

The VADAR results showed that the mean hydrogen bond distances and energy, mean helix phi parameters and mean Chi Gauche values in the FexB model were similar to the MdfA crystal structure data. The mean residue volume of MdfA and FexB model were 132.6 Å and 134.6 Å respectively, which indicates very good packing density of protein model. The structural details from the VADAR server are shown in Table 3. The 3-D structure of FexB model share the same overall fold as MdfA, with secondary structural elements mainly comprising of alpha-helices.The structure comprises of N- and C-terminal domains, each contributing to the catalytic site in between them. The structural superimposition of FexB model and MdfA indicated RMSD of 2.63 Å corresponding to the backbone atoms. The schematic representation of the structural overlay that highlights the

conservation in the overall structure is shown in Fig.4a and the mutation of ALA30 and SER93 amino acid residues in FexB model is shown in Fig.4b.

Table. 3 Structural characteristics and features of MdfA and FexB model from VADAR server

Protein	MHBD(Å)	MHBE	MHPh	MHPs	MCG+	MCG-	MRV(Å3)	TV(Å3)
MdfA	2.2	-1.6	-67.7	-36.9	-69.0	54.8	132.6	51855.3
FexB	2.2	-1.7	-65.6	-40.1	-67.8	69.2	134.6	63138.2

MHBD - Mean hbond distance; MHBE - Mean hbond energy; MHPh - Mean Helix Phi; MHPs – Mean Helix Psi; MCG+ - Mean Chi Gauche+;MCG- - Mean Chi Gauche-; MRV - Mean residue volume; TV - Total volume (packing)

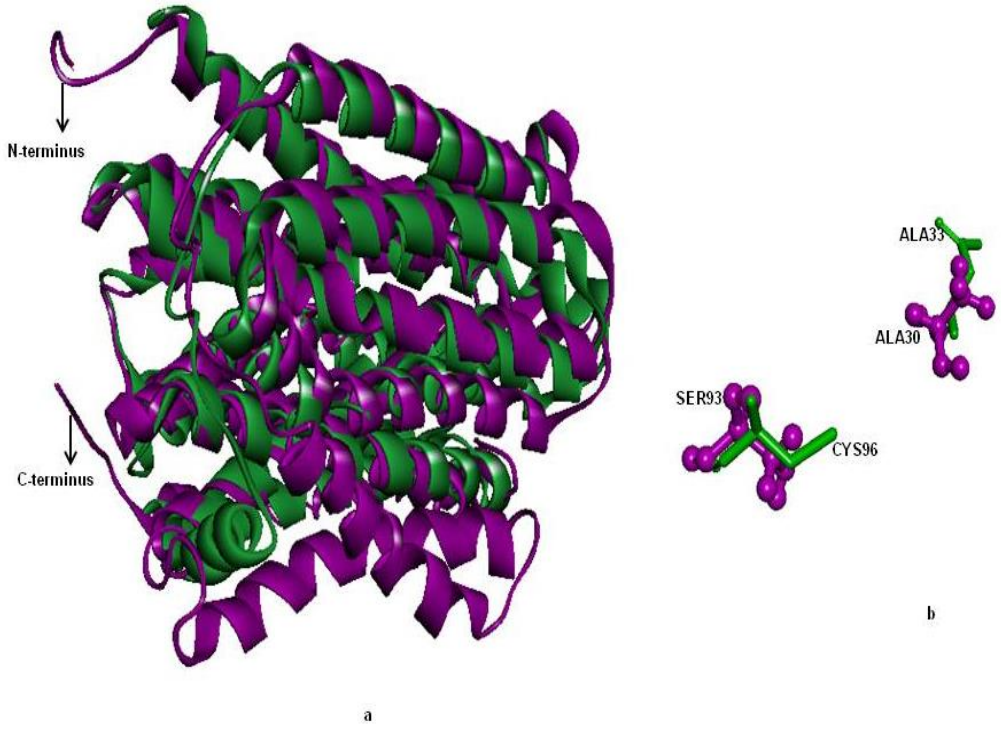

Fig.4 A schematic representation of (**a**) the structural overlay corresponding to the FexB model (*magenta*) and MdfA(*green*); (**b**) structural overlay showing the mutation of ALA30 and SER93 amino acid residues (ball and stick model) in FexB model that are present at the equivalent position of ALA33 and CYS96 in MdfA

3.3 Binding pocket identification

The binding pocket in FexB model and MdfA were identified using CASTp calculation server. Here, we have selected the largest cavity from the displayed structure as the binding pocket in both FexB as well as MdfA. The Clm binding pocket in FexB was similar to MdfA and was situated between the N- and C-terminal domains. The comparison of active site residues of both structures is highly conserved with residues ASP31, MET32, PRO35, LEU62, ARG109, GLN112, GLY113, ILE139, ALA144, PRO155, GLY154, GLY158, LEU165, TRP167, ILE177, ILE180, GLY184, GLN186, MET189, PRO190, ILE211, ILE213,GLY216, PHE218, GLY221, GLY229, SER232, ALA245,

ILE247 and LEU302 (numbered as per FexB). However, binding pocket of FexB was large (Area: 5226.5; Volume: 8792.6) (Fig.5a) when compared to MdfA(Area :1978.6; Volume:3930) (Fig.5b**)**. It has been observed that the substrate binding capacity is affected in proteins that are associated with large binding site [46]. Therefore, we hypothesize that large binding pocket in FexB protein may be responsible for its resistance towards Clm.

Fig.5 Catalytic active sites of (**a)** Fexb model; (**b)** MdfA predicted by CASTp calculations, *cyan* colored region represents the active site cavity

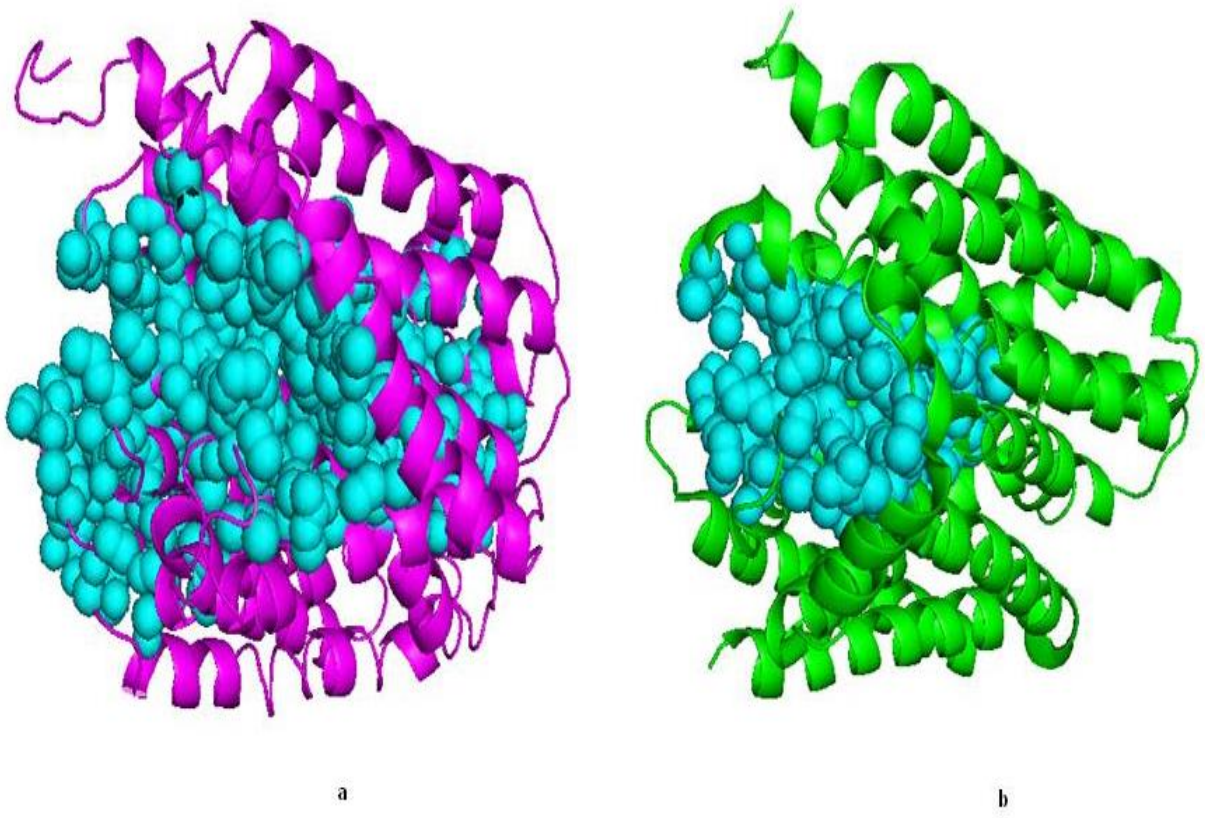

3.4 Docking Analysis

The docking was carried out using Autodock Vina by removing Clm from MdfA, and then redocking it into the protein, as well as into the modeled structure of FexB. The best docking mode was selected based on the orientation of the ligand in the active site and docking score. The results showed that binding energies were found to be -6.2 and -5.5 kcal/mol^{-1} for MdfA-Clm and FexB-Clm complexes respectively (Table 4). The intermolecular hydrogen bonds in the complexes were also analysed and it has been observed that MdfA-Clm formed two hydrogen bonds whereas FexB-Clm formed only one hydrogen bond. Fig.6a shows that the side chain NH of ASN33 forms hydrogen bond with oxygen of fourth carbon atom of Clm (NH....O4) and the OH group of ASP34 forms hydrogen bond

with oxygen of fifth carbon atom of Clm (OH....O5) in MdfA. On the other hand, the side chain OH of THR151 forms hydrogen bond with oxygen of fifth carbon atom of Clm (OH....O5) in FexB as shown in Fig.6b.

Fig.6 Superimposed structures of docked Clm (ball and stick) into active site (**a**) MdfA, (**b**) FexB. The color representation is as follows: original crystal structure Clm (ball and stick is colored by atom type) carbon (*grey*), protein carbon (*grey*), oxygen (*red*), nitrogen (*blue*), sulfur (*yellow*), and chlorine (*green*). The docked Clm in MdfA is shown in *blue* and *cyan* in FexB model. The active site residues are colored by atom type in MdfA and *magenta* in FexB model. The hydrogen bonds between the donor and acceptor atoms are shown in *red* broken lines

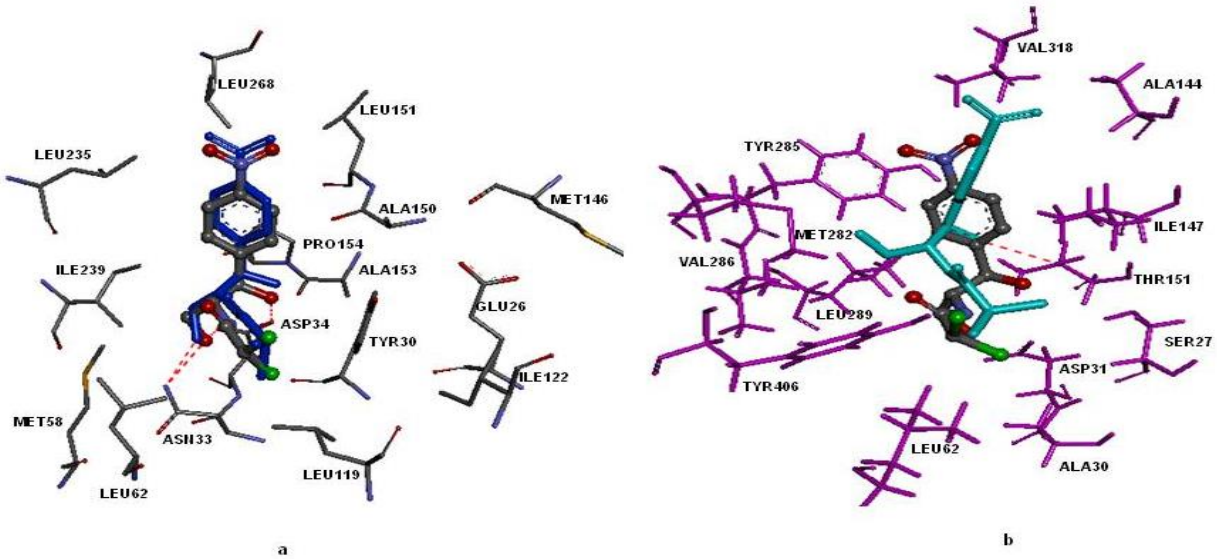

Table. 4 Comparison of Binding energies (in kcal mol-1) predicted by Autodock Vina between MdfA and FexB model after docking of CLM along with amino acid residues involved in H-bonding

Inhibitor	Protein	Binding affinity in kcal mol-1	Amino acids involved in H-bonding
Clm	MdfA	-6.2	ASN33, ASP34
Clm	FexB	-5.5	THR151

3.5 MD calculations

We have used GROMACS package 4.5.4 and performed MD calculations for analysing the RMSD, Root Mean Square Fluctuations (RMSF) and Radius of gyration (Rg) of the protein-ligand complex from MdfA and FexB. From the RMSD plots, we can analyze the conformational changes of all atom positions in the protein-ligand complex. The Cα atoms of protein RMSD vs Time showed some changes in the initial couple of nanoseconds. After equilibration at 2ns, MdfA showed minimum deviation leading to a RMSD of 0.2 nm while the FexB structure exhibited higher deviation leading to a RMSD of 0.4 nm at 10 ns of simulation (Fig. 7a). Similarly, we have also analyzed the conformational variations of both structures in complex with Clm. From the MD simulations trajectory, it has been observed that both protein complexes showed fluctuations upto 3 ns. The RMSD of MdfA-Clm was found to be 0.15 nm while FexB-Clm showed higher deviation with a RMSD of 0.25 nm (Fig.7b), indicating its conformational changes upon Clm binding.

Fig.7 RMSD vs. Time plots obtained from 10 ns of MD simulations. (**a**) Cα atoms of MdfA (*black*); FexB model (*red*); (**b**) MdfA-Clm complex(*black*), FexB-Clm complex(*red*)

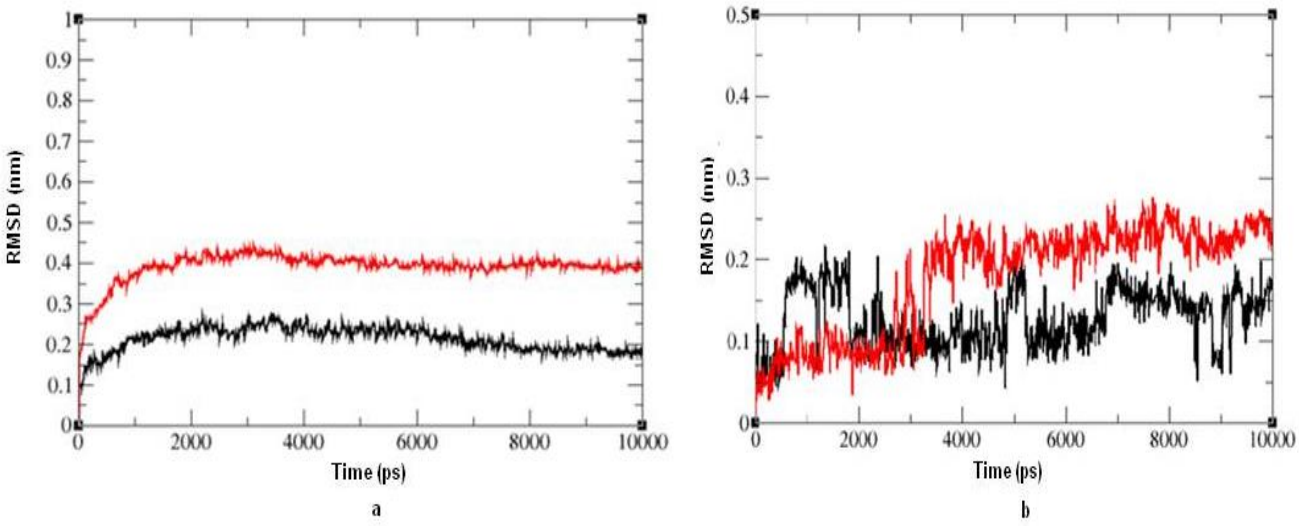

The Rg of MdfA was found to be 2.04nm while that of FexB was 2.10 nm after 10 ns of simulation (Fig. 8). Furthermore, RMSF analysis was carried out to better understand the fluctuation behaviour of binding residues of both MdfA and FexB structures. Majority of the active site residues of protein-ligand complex had RMSF values less than 0.4 nm with respect to MdfA. However, FexB protein revealed more residue fluctuations and degrees of flexibility when compared to MdfA (Fig. 9). Thus, this indicates the lack of FexB involvement in binding with Clm.

Fig.8 Radius of gyration (Rg) of all Cα atoms vs. Time plot from 10 ns of MD simulations. MdfA (*black*); FexB model (*red*)

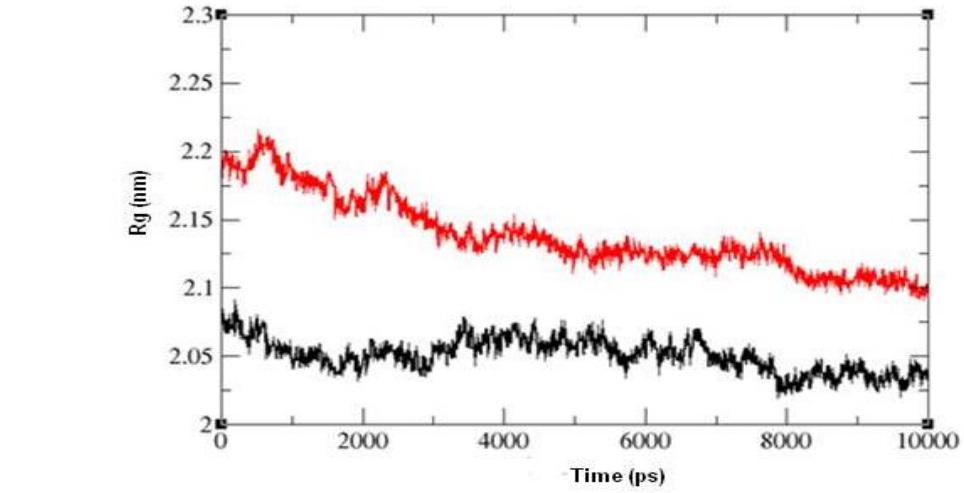

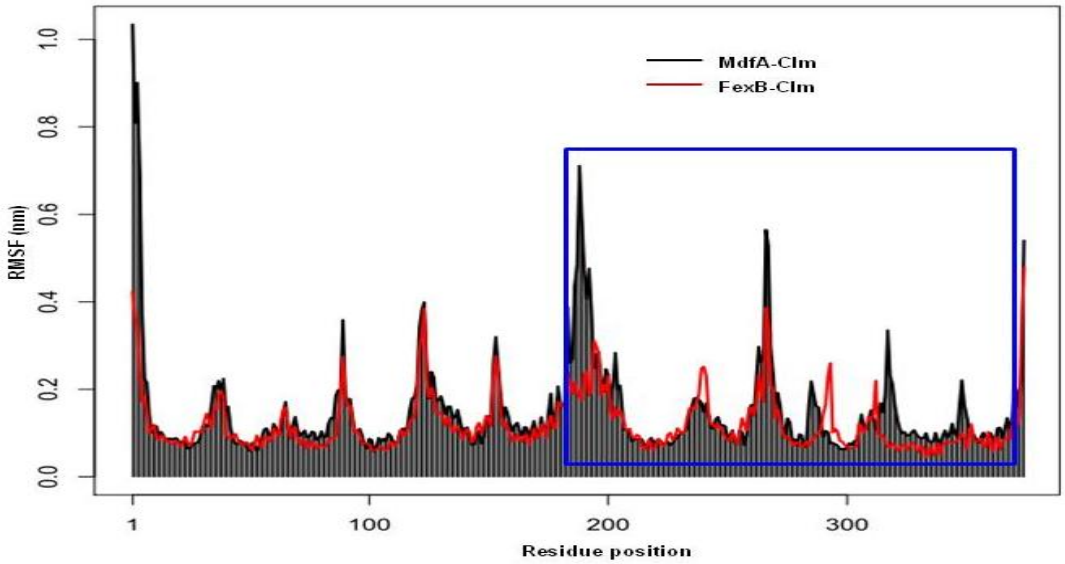

Fig. 9 RMSF of the whole residues in MdfA-Clm complex(*black*) and FexB-Clm complex(*red*). Specifically, the region comprising active site residues, region 200-400 (marked in blue box), shows more fluctuation of residues in the case of FexB-Clm complex as compared to MdfA-Clm complex

DISCUSSION

The main objective of the current study was to build the *in silico* 3D structure model of FexB protein with its MdfA homolog and to analyze the molecular mechanism of Clm drug resistance conferred by FexB protein using molecular docking followed by molecular dynamics simulations. Sequence

analysis revealed the presence of ASN33ALA and CYS96SER mutation in FexB protein thereby affecting its binding capacity with Clm. Our results were in agreement with the experimental study [13] which states that mutation of ASN33 to ALA and CYS96 to SER lost most of the binding ability towards Clm. The comparison of conserved motif analysis of FexB with MdfA revealed that motif-B is totally conserved whereas motif-C and D were partially conserved. Further, we have identified negatively charged C-terminal part along with two small grooves in FexB that might provide some possible target sites and can be considered when developing novel FexB inhibitors against Clm. Based on the crystal structure of MdfA, a successful 3D structural model was constructed for FexB protein by using homology modeling method. Despite of the low sequence similarity between the two proteins, we have observed that the overall fold of the FexB model was found to be highly comparable with MdfA. In addition, we have identified large binding pocket in FexB protein when compared to MdfA that could further aid in designing new drug molecules. Docking studies showed the presence of decreased intermolecular interactions and was significantly affected due to the presence of large binding site in FexB protein as a result of which affinity towards Clm is decreased leading to its resistance. MD simulations also demonstrated conformational changes of FexB-Clm complex that could be related to the development of drug resistance.

4. CONCLUSION

Taken together, we believe that the FexB-3D model could be used for the rational design of more robust and effective drugs that will target in countering the resistance conferred to Clm. These results are expected to be helpful and valuable in the development of more efficient drugs against antibiotic resistant micro-organisms and their mutants.

CONFLICTS OF INTEREST

None

ACKNOWLEDGEMENT

The author would like to thank the Centre for Modelling Simulation and Design (CMSD), University of Hyderabad, for providing access to carry out the molecular dynamics calculations.

ABBREVIATIONS:

Clm	Chloramphenicol
Fm	Florfenicol
1D	One-Dimensional
3D	Three-Dimensional
MD	Molecular Dynamics
PDB	Protein Data Bank
GRAVY	Grand Average of Hydropathy
II	Instability Index
VADAR	Volume Area Dihedral Angle Reporter
SAVES	Structure Analysis and Verification Server
NVT	Normal Volume Temperature
NPT	Normal Pressure Temperature
LJ	Lennard–Jones
MFS	Major Facilitator Superfamily
pH	Measure of acidity; negative logarithm of proton concentration
pI	Isoelectric point
Cα	C-alpha

REFERENCES

1. Poole K (2002) Mechanisms of bacterial biocide and antibiotic resistance. J Appl Microbiol 92: 55S-64S
2. Wright GD (2003) Mechanisms of resistance to antibiotics. Curr Opin Chem Biol 7: 563-569
3. McDermott PF, Walker RD, White DG (2003) Antimicrobials: modes of action and mechanisms of resistance. Int J Toxicol 22: 135-143
4. Hogan D, Kolter R (2002) Why are bacteria refractory to antimicrobials? Curr Opin Microbiol 5: 472
5. Normark BH and Normark S (2002) Evolution and spread of antibiotic resistance. J Intern Med 252: 91-106
6. Liebana E, Carattoli A, Coque TM, Hasman H, Magiorakos AP,Mevius D, et al (2013) Public health risks of enterobacterial isolates producing extended-spectrum beta-lactamases or AmpC beta-lactamases in food and food-producing animals: an EU perspective of epidemiology, analytical methods, risk factors, and control options. Clin Infect Dis 56:1030-1037
7. Burkholder PR (1947) Chloromycetin a new antibiotic from a soil actinomycete. Science 106:417
8. Vinning LC, Stuttard C (1995) Chloramphenicol. Biotechnology 28:505-530
9. Shaw WV (1983) Chloramphenicol acetyltransferase, enzymology and molecular biology. Crit Rev Biochem 14:1-46
10. Yao JDC and Moellering Jr RC (1999) Manual of Clinical Microbiology. In: (Murray, PR, Baron, EJ, Pfaller, MA,Tenover, FC and Yolken, RH) pp. 1474–1505 ASM Press,Washington, D.C.
11. Soback S, Paape MJ, Filep R, Varma KJ (1995) Florfenicol pharmacokinetics in lactating cows after intravenous, intramuscular and intramammary administration. J Vet Pharmacol Ther 18:413- 417
12. Schwarz S, Kehrenberg C, Doublet B, Cloeckaert A (2004) Molecular basis of bacterial resistance to chloramphenicol and florfenicol. FEMS Microbiol Rev 28:519-542
13. Liu H, Wang Y, Wu C, Schwarz S, Shen Z, Jeon B, Ding S, Zhang Q, Shen J (2012) A novel phenicol exporter gene, fexB, found in enterococci of animal origin. J Antimicrob Chemother 67:322-325
14. Hofmann K and Stoffel W (1993) TMbase - A database of membrane spanning proteins segments. Biol Chem Hoppe-Seyler **374:**166
15. Wilkins MR, Gasteiger E, Bairoch A, Sanchez JC, Williams KL, Appel RD, Hochstrasser DF (1999) Protein identification and analysis tools in the ExPASy server. Methods Mol Biol 112:531-552
16. Laskowski RA, Chistyakov VV, Thornton JM (2005) PDBsum more: new summaries and analyses of the known 3D structures of proteins and nucleic acids. Nucleic Acids Res 33:D266 - D268
17. Olsson MHM, Søndergaard CR, Rostkowski M, Jensen JH (2011) PROPKA3: consistent treatment of internal and surface residues in empirical pKa predictions. J Chem Theory Comput 7:525-537

18. Dolinsky TJ, Nielsen JE, McCammon JA, Baker NA (2004) PDB2PQR: an automated pipeline for the setup, execution, and analysis of Poisson-Boltzmann electrostatics calculations. Nucleic Acids Research 32: W665-W667
19. Baker NA, Sept D, Joseph S, Holst MJ, McCammon JA (2001) Electrostatics of nanosystems: application to microtubules and the ribosome. Proc Natl Acad Sci USA 98:10037-10041
20. Altschul SF, Gish W, Miller W, Myers EW, Lipman DJ (1990) Basic local alignment search tool. Journal of Molecular Biology 215: 403-410
21. Berman HM, Westbrook J, Feng Z, Gilliland G, Bhat, TN, Weissig H, Bourne PE (2000) The protein data bank. Nucleic Acids Research 28: 235-242
22. Jie H, Yan Z, Ming L, Yue L, Junping F, Xianping W, Yongfang Z, Xuejun CZ (2015) Substrate-bound structure of the *E. coli* multidrug resistance transporter MdfA. Cell Research 25:1060-1073
23. Sievers F, Wilm A, Dineen D, Gibson TJ, Karplus K, Li W, Lopez R, McWilliam H, Remmert M, Soding J, Thompson JD, Higgins DG (2011) Fast, scalable generation of high-quality protein multiple sequence alignments using Clustal Omega. Mol Syst Biol 7:539
24. Arthur D, Vassilvitskii S (2007) k-means++: the advantages of careful seeding. Proceedings of the Eighteenth Annual ACM-SIAM Symposium on Discrete Algorithms. pp 1027–1035
25. Jianyi Y, Yang Z (2015) I-TASSER server: new development for protein structure and function predictions. Nucleic Acids Research 43: W174-W181
26. Willard L, Ranjan A, Zhang H, Monzavi H, Boyko RF, Sykes BD, Wishart DS (2003) VADAR: A web server for quantitative evaluation of protein structure quality. Nucleic Acids Research 31: 3316-3319
27. Laskowski RA, MacArthur MW, Moss DS, Thornton JM (1993) PROCHECK: A program to check the stereochemical quality of protein structures. Journal of Applied Crystallography 26:283-291
28. Lüthy R, Bowie JU, Eisenberg D (1992) Assessment of protein models with three-dimensional profiles. Nature 356: 83-85
29. Ramachandran GN, Ramakrishnan C, Sasisekharan V (1963) Stereochemistry of polypeptide chain configurations. Journal of Molecular Biology 7:95-99
30. Dundas J, Ouyang Z, Tseng J, Binkowski A, Turpaz Y, Liang J (2006) CASTp: Computed atlas of surface topography of proteins with structural and topographical mapping of functionally annotated residues. Nucleic Acids Res 34:W116-118
31. Trott O, Olson AJ (2010) AutoDockVina: improving the speed and accuracy of docking with a new scoring function, efficient optimization and multithreading. J Comput Chem 2:455-461
32. Hess B, Kutzner C, van der Spoel D, Lindahl, E (2008) GROMACS 4: Algorithms for highly efficient, load-balanced, and scalable molecular simulation. Journal of Chemical Theory and Computation 4:435-447
33. Van Der Spoel D, Lindahl, E, Hess B, Groenhof G, Mark AE, Berendsen H J (2005) GROMACS: Fast, flexible, and free. Journal of Computational Chemistry 26:1701-1718

34. Bussi G, Donadio D, Parrinello M (2007) Canonical sampling through velocity rescaling. The Journal of Chemical Physics 126: 014101
35. Parrinello M, Rahman A (1981) Polymorphic transitions in single crystals: A new molecular dynamics method. Journal of Applied Physics 52:7182-7190
36. Hess B, Bekker H, Berendsen HJC, Fraaije JGEM (1997) LINCS: A linear constraint solver for molecular simulations. Journal of Computational Chemistry 18:1463-1472
37. Darden T, York D, Pedersen L (1993) Particle mesh Ewald: An N·log(N) method for Ewald sums in large systems. The Journal of Chemical Physics 98:10089-10092
38. Essmann U, Perera L, Berkowitz ML, Darden T, Lee H, Pedersen LG (1995) A smooth particle mesh Ewald method. The Journal of Chemical Physics 103:8577-8593
39. Humphrey W, Dalke A, Schulten K (1996) VMD - visual molecular dynamics. J Mol Graph 14:33–38
40. Paulsen IT, Brown MH, Skurray RA (1996) Proton-dependent multidrug efflux systems. Microbiol Rev 60:575-608
41. Pasrija R, Banerjee D, Prasad R (2007) Structure and function analysis of CaMdr1p, a major facilitator superfamily antifungal efflux transporter protein of Candida albicans: identification of amino acid residues critical for drug/H+ transport. Eukaryotic Cell 6:443-453
42. Fluman N, Ryan CM, Whitelegge JP, Bibi E (2012) Dissection of mechanistic principles of a secondary multidrug efflux protein. Mol Cell 47:777-787
43.Edgar R, Bibi E (1999) A single membrane-embedded negative charge is critical for recognizing positively charged drugs by the Escherichia coli multidrug resistance protein MdfA. EMBO J 18:822-832
44. Sigal N, Fluman N, Siemion S, Bibi E (2009) The secondary multidrug/proton antiporter MdfA tolerates displacements of an essential negatively charged side chain. J Biol Chem 284:6966-6971
45. Adler J, Bibi E (2005) Promiscuity in the geometry of electrostatic interactions between the Escherichia coli multidrug resistance transporter MdfA and cationic substrates. J Biol Chem 280:2721-2729
46. Ramulu HG, Adindla S, Guruprasad L (2006) Analysis and Modeling of mycolyl-transferases in the CMN group. Bioinformation. 5:161-191

SUPPLEMENTARY INFORMATION

Fig. S1 Schematic representation of 14 Transmembrane domains in FexB protein sequence from Tmpred prediction server

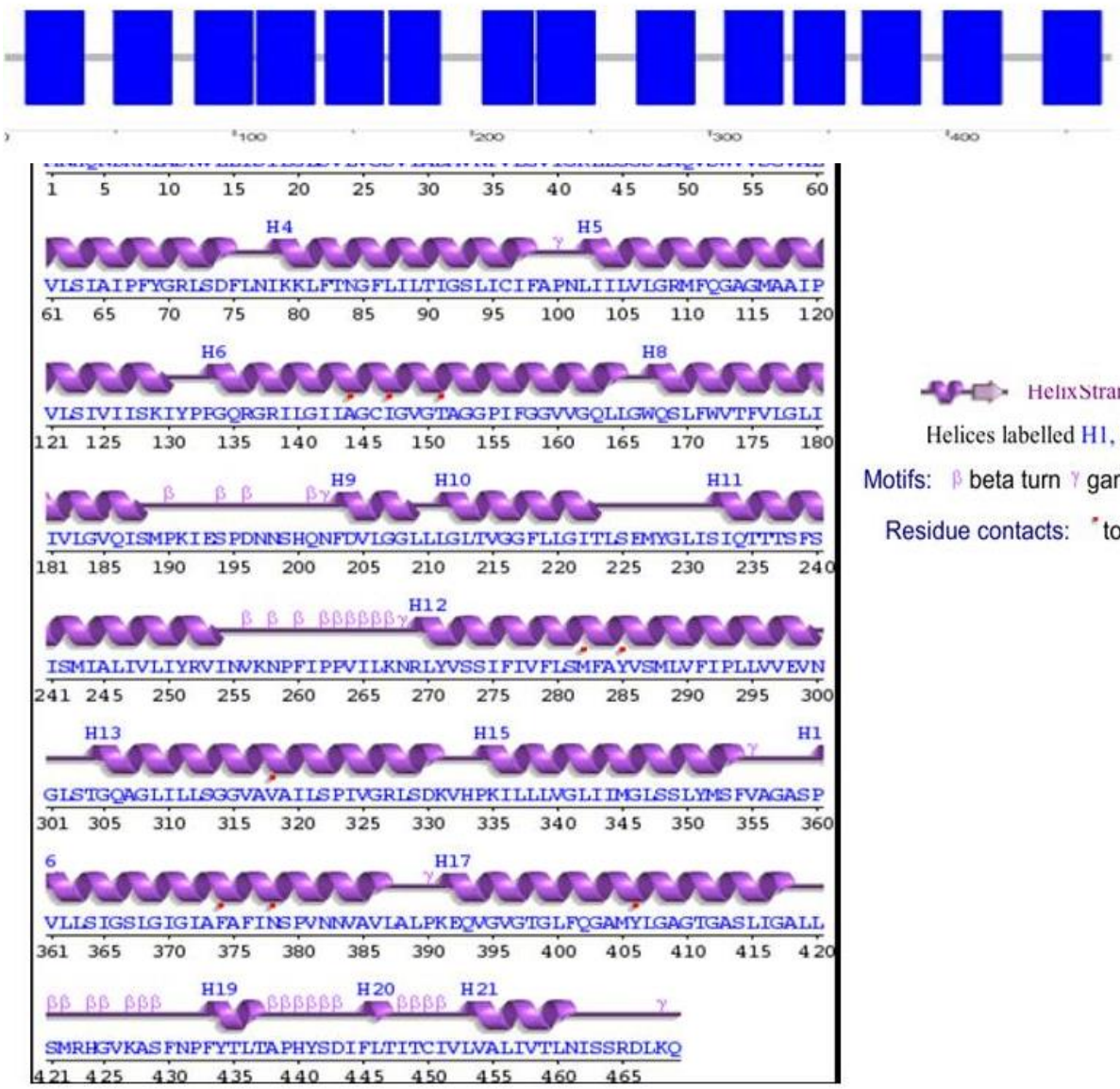

Fig. S2 Prediction of the secondary structure of FexB protein sequence from PDBsum server

Fig. S3 Representation of the surface electrostatic potential of MdfA and FexB model. (**a)** MdfA; (**b)** FexB. For each structure, the front view is depicted on the left, the side view on the right. A negatively charged C-terminal part along with two small grooves that are specific to FexB model is circled in *green*. PDB2PQR server [18] was used to calculate the electrostatic potentials